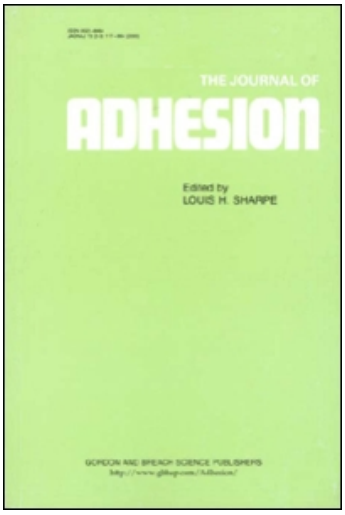

The Journal of Adhesion
Publication details, including instructions for authors and subscription information:
http://www.informaworld.com/smpp/title~content=t713453635

The Effect of Cure Conditions on a Rubber-Modified Epoxy Adhesive

S. J. Shaw[a]; D. A. Tod[a]
[a] Ministry of Defence, Royal Armament Research & Development Establishment, Abbey, Essex, UK

To cite this Article Shaw, S. J. and Tod, D. A.(1989) 'The Effect of Cure Conditions on a Rubber-Modified Epoxy Adhesive', The Journal of Adhesion, 28: 4, 231 — 246
To link to this Article: DOI: 10.1080/00218468908030172
URL: http://dx.doi.org/10.1080/00218468908030172

J. Adhesion, 1989, Vol. 28, pp. 231–246
Reprints available directly from the publisher
Photocopying permitted by license only

Printed in the United Kingdom

The Effect of Cure Conditions on a Rubber-Modified Epoxy Adhesive†

S. J. SHAW and D. A. TOD

Ministry of Defence, Royal Armament Research & Development Establishment, Waltham Abbey, Essex, UK

(Received February 9, 1988; in final form January 23, 1989)

The effect of cure conditions on the mechanical properties of a piperidine-cured, rubber-modified epoxy is described. The results obtained reveal that variations in cure conditions (temperature and time) have a pronounced influence on the mechanical behaviour, in particular the fracture energy obtained in both bulk and adhesive joint form. Techniques such as dynamic mechanical spectroscopy and scanning electron microscopy have been employed in an attempt to explain the trends.

KEY WORDS Piperidine cure; mechanical properties; fracture toughness; cure conditions; dynamic mechanical spectroscopy; scanning electron microscopy.

1 INTRODUCTION

Rubber-modified epoxy resins are nowadays employed extensively in structural adhesive formulations where high levels of toughness are achieved with only minor reductions in other important properties such as modulus and glass transition temperature.

Many factors have been shown to influence the mechanical properties of rubber-modified epoxies. Notable examples include the type and concentration of the rubber-modifier together with the nature of the curing agent employed.[1–4] Although cure conditions (temperature and time) are known to influence the mechanical properties of unmodified epoxies, it is only recently that detailed attempts have been made to study the effects of these variables with rubber-modified formulations.[5,6]

For various reasons, many of the fundamental investigations conducted on modified epoxies have used formulations employing piperidine as the curing agent.[7–11] In the majority of these studies a rather prolonged cure regime of 16 hours at 120°C has been employed, this resulting from convenience, rather than a

† Presented at the International Conference, "Adhesion '87," of the Plastics and Rubber Institute held at York University, England, September 7–9, 1987.

technological requirement; 16 hours roughly equates with an overnight cure. In an attempt to determine whether this lengthy cure profile could be relaxed, a study was initiated to determine the effects of cure conditions on the mechanical behaviour of a piperdine cured rubber-modified epoxy. This paper discusses some of the results obtained.

2 EXPERIMENTAL

2.1 Materials

The epoxy resin employed was a liquid diglycidyl-ether of bisphenol A (DGEBA) having an epoxy equivalent weight of approximately 190 g mole^{-1}. The curing agent was piperidine and the rubber modifier employed was a carboxyl-terminated butadiene-acrylonitrile rubber (CTBN) having an acrylonitrile content of 17% and a molar mass of 3500 g mol^{-1}. The above constituents were employed in the following proportions throughout this work:

DGEBA	100 pbw
CTBN	15 pbw
Piperidine	5 pbw

The above formulation was prepared by initially adding the required quantity of CTBN to the resin followed by hand-mixing for approximately ten minutes. The resultant mixture was then raised to a temperature of 70°C in a water bath and stirred for five minutes with an electric stirrer, followed by degassing in a vacuum oven at 60°C. After cooling to 30°C, the piperidine was added and the mixture gently stirred so as to minimise air entrapment. The formulation at this stage was then ready either for casting into a 6 mm thick mould so as to produce sheets for bulk mechanical property studies or for adhesive joint preparation.

2.2 Bulk mechanical property studies

A casting technique using a stainless steel mould was employed to prepare bulk mechanical property test specimens. Prior to casting, the inner surfaces of the mould were treated with a mould release agent, followed by heating to a temperature of 120°C. Immediately following this, the epoxy formulation, at a temperature of 60°C, was cast into the mould and cured in an air-circulating oven, followed by gradual cooling. A total of nine cure temperature/time conditions were investigated and are shown in Table I.

On removal from the mould, the cured sheets were either cut into compact tension specimens for fracture characterisation (Figure 1) or rectangular plates measuring 20 mm by 130 mm for modulus determination by a three-point-bend technique.

For fracture evaluation, the compact tension specimens were subjected to a pre-cracking procedure whereby a sharp pre-crack was introduced by carefully

TABLE I
Cure temperature/time conditions employed

Temperature (°C)	Time (hours)
120	2
120	4
120	6
140	2
140	4
140	6
160	2
160	4
160	6

tapping a fresh razor blade into the base of the saw-cut. This caused a natural crack to grow for a short distance ahead of the blade. The specimens were then mounted in a mechanical testing machine and fractured at 20°C at a constant crosshead displacement rate of 1 mm min^{-1}.

Values of stess intensity factor, K_{Ic}, were calculated from the expression,[12]

$$K_{Ic} = \frac{P_c}{BW^{1/2}} Q \tag{1}$$

where P_c = maximum load attained during crack propagation, W = width of the specimen as indicated in Figure 1, B = specimen thickness and Q = geometry

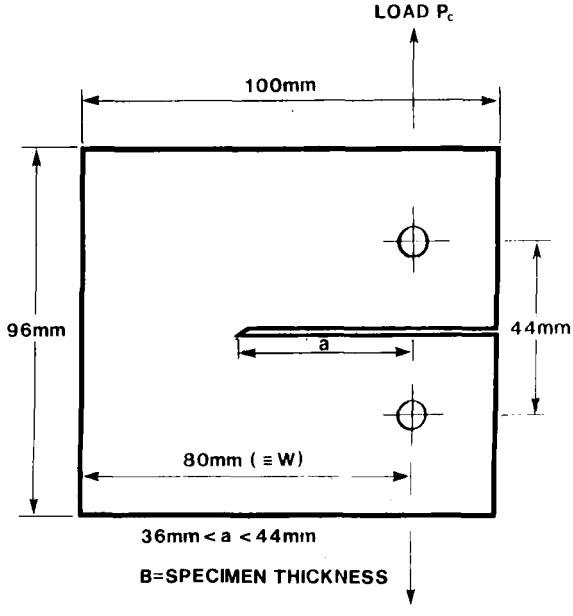

FIGURE 1 Compact tension specimen.

factor given by,

$$Q = 29.6\left(\frac{a}{w}\right)^{1/2} - 185.5\left(\frac{a}{w}\right)^{3/2} + 655.7\left(\frac{a}{w}\right)^{5/2} - 1017\left(\frac{a}{w}\right)^{7/2} + 638.9\left(\frac{a}{w}\right)^{9/2}$$

where a = crack length.

The critical stress intensity factor, K_{Ic}, values were converted to fracture energy, G_{Ic}, using the equation

$$G_{Ic} = \frac{K_{Ic}^2}{E}(1 - \nu^2) \tag{2}$$

where E is Young's modulus and ν is Poisson's ratio (assumed to be 0.35).

Modulus measurements were conducted using a three-point-bend technique according to ASTMD790-71 at 20°C and 1 mm min^{-1} crosshead displacement.

Dynamic mechanical studies were conducted using a Rheometrics mechanical spectrometer on rectangular specimens, measuring 85 × 10 × 6 mm, obtained from the cast sheets. Measurements were taken at approximately 5°C intervals between −160°C and 150°C.

2.3 Adhesive joint fracture studies

The specimen geometry employed for the adhesive joint fracture tests was a contoured-double-cantilever-beam joint, as shown schematically in Figure 2. The substrate material employed was mild steel, to specification British Standard 970 EN3B, which was machined into cantilever beams 308 mm long with the height, h, ranging from 15.8 to 51 mm. Prior to bonding, the mild steel surfaces were firstly subjected to liquid and vapour-degreasing in 1,1,1-trichloroethane, followed by grit-blasting with 180–220 mesh alumina. This was followed by a further identical degreasing process. Two pre-treated beams were pressed down firmly on a glass sheet covered with double-sided adhesive tape. Polystyrene or, in certain cases, brass spacers were positioned at each end of the specimen to control bond thickness and provide a casting reservoir for the adhesive. A piece of PTFE tape the width of the joint and about 60 mm long by 0.08 mm thick was placed at the loading end of the specimen so as to assist starter crack formation.

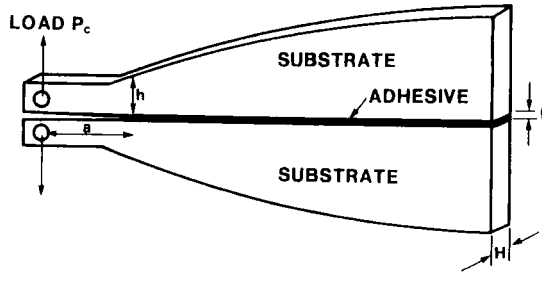

FIGURE 2 Contoured double cantilever beam specimen.

The complete assembly was then preheated to 160°C in an air circulating oven. The rubber-modified epoxy formulation, at a temperature of 60°C, was then cast into the reservoir and the assembly returned to the oven for a cure cycle of 6 hours at 160°C, followed by slow cooling. Subsequent fracture experiments were conducted at 20°C at a constant crosshead displacement rate of 1 mm min^{-1}. Variables studied in this programme were joint width, H, ranging from 6 to 49 mm and bond line thickness, t, ranging from approximately 0.5 to 2.0 mm.

Values of adhesive fracture energy, G_{Ic} (joint) were determined from the relationship,[13]

$$G_{Ic}(\text{joint}) = 4P_c^2 m / E_S H^2 \tag{3}$$

where P_c = load at crack initiation, E_s = modulus of the substrate, H = specimen width and m is a geometry factor.

2.4 Fractography

Fracture surfaces were studied using a JEOL T300 scanning electron microscope at a beam current and accelerating voltage of approximately 175 mA and 20 kV respectively. Prior to examination, surfaces were coated with a thin evaporated layer of gold/palladium so as to enhance conductivity and prevent charging.

3 RESULTS AND DISCUSSION

3.1 Bulk properties

Values of fracture energy, G_{Ic}, obtained from the compact tension specimens are shown as a contour diagram in Figure 3. Before discussing this figure, it would be useful to describe briefly the contour technique used to present the data. The technique is based on the data given in Table II, which shows G_{Ic} values obtained

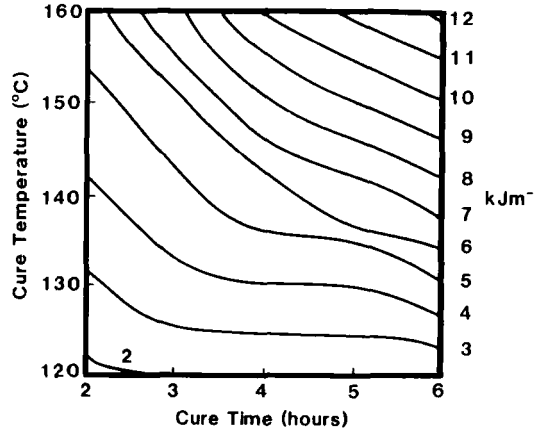

FIGURE 3 Bulk fracture energy contour diagram.

TABLE II
Cure temperature/time combinations employed and G_{Ic} values obtained

Temperature (°C)	Time (hours)	G_{Ic} (kJm^{-2})
120	2	1.75
120	4	2.20
120	6	2.15
140	2	3.79
140	4	5.63
140	6	7.62
160	2	5.52
160	4	10.15
160	6	12.12

from the nine cure schedules employed in this programme. Figure 4 shows these nine G_{Ic} values plotted as a matrix construction having axes of cure temperature as a function of cure time. The contour diagram is obtained by simply drawing straight lines between each of the data points obtained, as indicated, and then assuming a linear change in properties (in this case G_{Ic}) between the data points. The contour lines are then simply obtained by linking together regions having identical G_{Ic} values. Although the linearity assumption just described could be a source of error, we feel that provided a sufficiently large amount of experimental data is employed in the contour construction, then the diagrams obtained provide a valuable and reasonably accurate insight into the way in which properties vary with cure conditions.

As indicated in Figure 3 and Table II, variations in cure temperature between 120 and 160°C over cure times ranging from 2 to 6 hours result in G_{Ic} changes between 1.75 and 12.12 kJm^{-2}, *i.e.* simply changing from 2 hours at 120°C to 6 hours at 160°C can increase fracture energy with this particular system approxim-

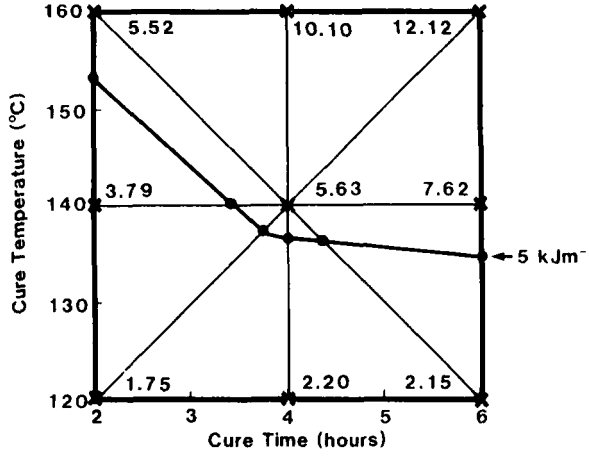

FIGURE 4 Contour diagram construction technique.

ately seven-fold. A statistical analysis employing a two-way analysis of variance has shown highly significant cure temperature and time effects. A highly significant cure temperature/time interaction has also been found which, upon further analysis, has been shown to be primarily due to the 120°C cure temperature data being "odd;" a subsequent two-way analysis of variance using only the 140 and 160°C data indicating a substantially reduced degree of significance. It is particularly interesting to note that the value of G_{Ic} previously obtained for an identical system cured for 16 hours at 120°C (the traditional cure regime) was approximately 1.7 kJm^{-2} which compares favourably with the fracture energy value obtained from a 2-hour cure time at the same temperature.[14] Thus, in no way can a relaxation in cure time be considered harmful in this case. Indeed, a significant reduction in cure time from the original 16 hours results in improved G_{Ic} values, particularly if cure temperature is raised.

A maximum G_{Ic} value of approximately 12 kJm^{-2} clearly provides doubt as to its validity in that the degree of crack tip plasticity producing the high toughness values could also lead to an invalid result. In an attempt to resolve this problem, load-displacement relations were obtained from the compact tension tests, and examined to assess plasticity effects by the standardised offset procedure.[12] Five such relationships are shown in Figure 5 for five of the nine cure conditions studied. In addition to allowing an assessment of the significance of plasticity related effects, the offset procedure allows for an estimate of the point at which crack propagation commences, thus providing the necessary data for calculation of K_{Ic} at the instant of crack propagation. As mentioned previously, as a matter of convenience, K_{Ic} values (and hence the G_{Ic} values given in Table II) were obtained using maximum load data. It is, therefore, of interest to employ the offset procedure to determine any major differences which may exist between the toughness parameters obtained from the two approaches. Since excellent accounts of this procedure exist elsewhere, no attempt will be made here to describe the main details. Instead, only the main data and conclusions obtained will be described. Table III shows the G_{Ic} values obtained from the two approaches, *i.e.* calculated at the instant of crack propagation and at maximum load.

Clearly, for specimens which exhibit load-displacement curves having significant curvature, a substantial difference between toughness values obtained at initiation and maximum load exists. Thus, it would appear that the maximum load data have a significant contribution from plasticity-related effects, particularly so at the higher cure temperatures.† An assessment of the load-displacement curves revealed no major plasticity contributions regarding the initial crack propagation data.

† It is of interest to note that, since the original presentation of this paper, Kinlock *et al.*, employing a cure condition of 6 hours at 160°C on a similar formulation, has agreed with the general observations described above, but with somewhat lower fracture energy values.[15] Since they took crack tip plasticity effects into account it is likely that this difference is attributable, partly at least, to the plasticity effects described above.

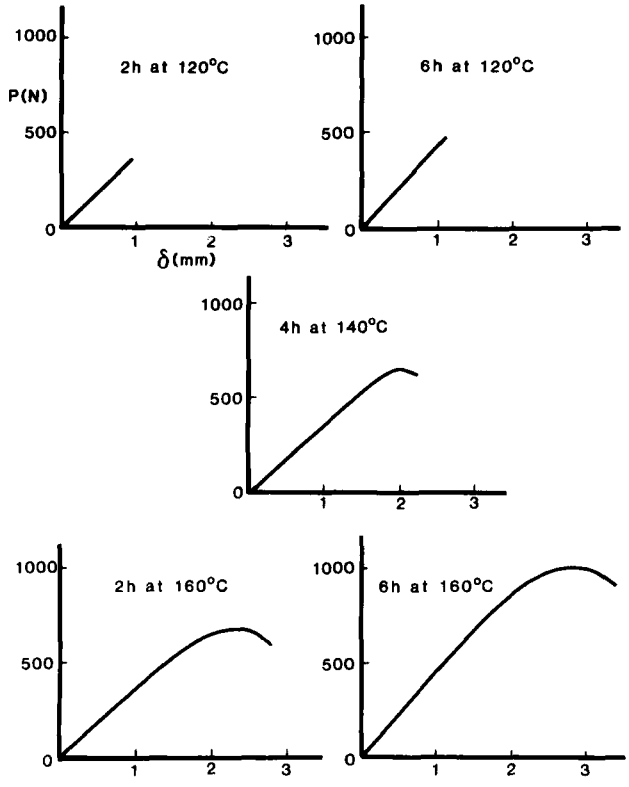

FIGURE 5 Load-displacement (P-δ) relationships for five of the cure conditions studied.

Although it is likely, therefore, that some of the data employed in the construction of the G_{Ic} contour diagram may not be entirely valid in terms of a linear elastic approach to fracture, it is clear that variations in cure conditions, particularly at temperatures approaching 160°C, are promoting a substantially enhanced toughness.

In addition, a specimen thickness of 6 mm may seem intuituvely low for such tough polymers, leading to the possibility of a substantial plane-stress contribu-

TABLE III
Comparisons of G_{Ic} values obtained at (a) instant of crack propagation and (b) maximum load.

Cure conditions (hrs/°C)	G_{Ic} (initiation) (kJm^{-2})	G_{Ic} (max. load) (kJm^{-2})	% overestimate
2/120	1.75	1.75	0
6/120	2.15	2.15	0
4/120	4.10	5.63	37
2/160	3.91	5.52	41
6/160	6.81	12.12	78

tion to toughness. However, previous work employing an identical toughened epoxy formulation cured for the traditional 16 hours at 120°C has shown that fracture energy is independent of specimen thickness at thicknesses between 1 and 50 mm.[14] This effect has been attributed to a two-phase morphology resulting in a toughening mechanism which produces a complex crack tip stress state in which the matrix never exhibits simple plane-stress or plane-strain behaviour under most conditions. Since this programme of work has shown that the two-phase morphology is maintained under all the cure conditions studied, it would seem unlikely that significant specimen thickness effects would exist for formulations cured under other time/temperature conditions.

Figure 6 shows the contour diagram constructed from flexural modulus data obtained from the rubber-modified epoxy cured under the nine cure regimes. As indicated, modulus variation as a function of cure temperature and time is rather complex. However, three main points are of importance. Firstly, for the cure temperature/time range shown, increasing cure temperature results in a reduced modulus. Although this would seem intuitively strange, it is of interest to note that similar behaviour has been observed by other workers, where free volume related effects have been considered responsible for this anomalous behaviour.[16–18] This, and other bulk property aspects, will be considered in more detail in a later publication. Secondly, despite the above, modulus does not vary substantially with cure conditions, so that the significant increases in toughness resulting from an increase in cure temperature do not result at the expense of modulus. Thirdly, it is of interest to note that the modulus value obtained from the traditional cure condition of 16 hours at 120°C, 2.57 Gpa,[14] fits reasonably well into the trends depicted in Figure 6.

Results obtained from dynamic mechanical experiments conducted on two

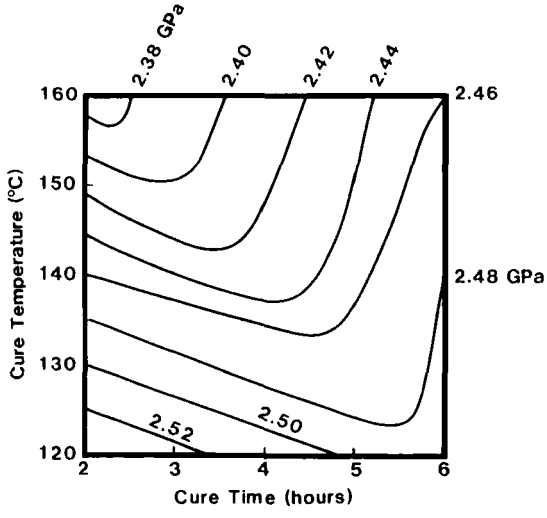

FIGURE 6 Flexural modulus contour diagram.

samples cured for 2 hours at 120°C and 6 hours at 160°C, *i.e.* exhibiting the lowest and highest fracture energy values respectively, are shown in Figure 7 with loss tangent, tan δ, plotted as a function of temperature. In both cases, the high temperature region is dominated by a peak at approximately 93°C, which can be attributed to the glass transition, T_g. This value compares favourably with that obtained by other workers for similar formulations. Note in particular that whilst the change in cure conditions has a negligible effect on T_g, it does appear to influence the width of the loss peak. Although it would be reasonable to assume that an increase in cure temperature could result in an increased T_g, Kinloch and co-workers have found the reverse effect, which they attributed to a reduction in matrix crosslink density.[15]

Both systems show a second, much smaller peak with a maximum tan δ at approximately −55°C. Relaxations in this temperature region are common with a wide range of epoxy systems. For unmodified epoxies, they are generally referred to as β relaxations and are believed to result from crankshaft rotations of glyceryl units, —CH_2—CH(OH)—CH_2—O—, in the epoxy matrix.[10,19–21] Complications, however, exist with rubber-modified epoxies since the elastometric component, CTBN, generally exhibits a glass transition in this temperature region. Consequently, for the data shown in Figure 7, the low temperature peak will be composed of both the β relaxation of the epoxy phase and the T_g of the rubber phase. As indicated, the cure variations clearly influence both the magnitude of the low temperature peak and the temperature at which it occurs which can almost certainly be attributed to differences in rubber phase volume between the two systems. It is perhaps of interest to note that, throughout this study, rubber modification has been shown to have no major effect on T_g, suggesting that most of the rubber phase separates prior to gelation with only a minimal amount remaining in the epoxy matrix. Since the rubbery phase is composed of both CTBN and epoxy derived species, the above findings would suggest that, since

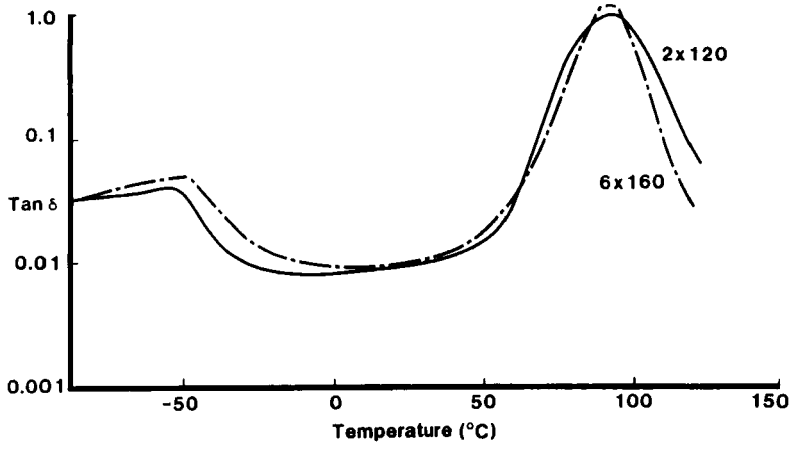

FIGURE 7 Loss tangent, tan δ, as a function of temperature for two cure conditions.

the initial CTBN concentration is maintained constant, cure variations change the relative amounts of each in the rubbery phase.

Figure 8 shows scanning electron micrographs for both the 2-hour × 120°C and 6-hour × 160°C systems. Both micrographs show a large number of holes at positions originally occupied by rubber particles. The mechanism responsible for the development of this topography has been discussed by the present authors and co-workers.[10] Differences between the two systems are clearly apparent, with the higher cure temperature/time (6 × 160) appearing to show substantially larger rubber particles than its reduced cure regime counterpart (2 × 120). Similar differences have been observed with transmission electron micrographs obtained

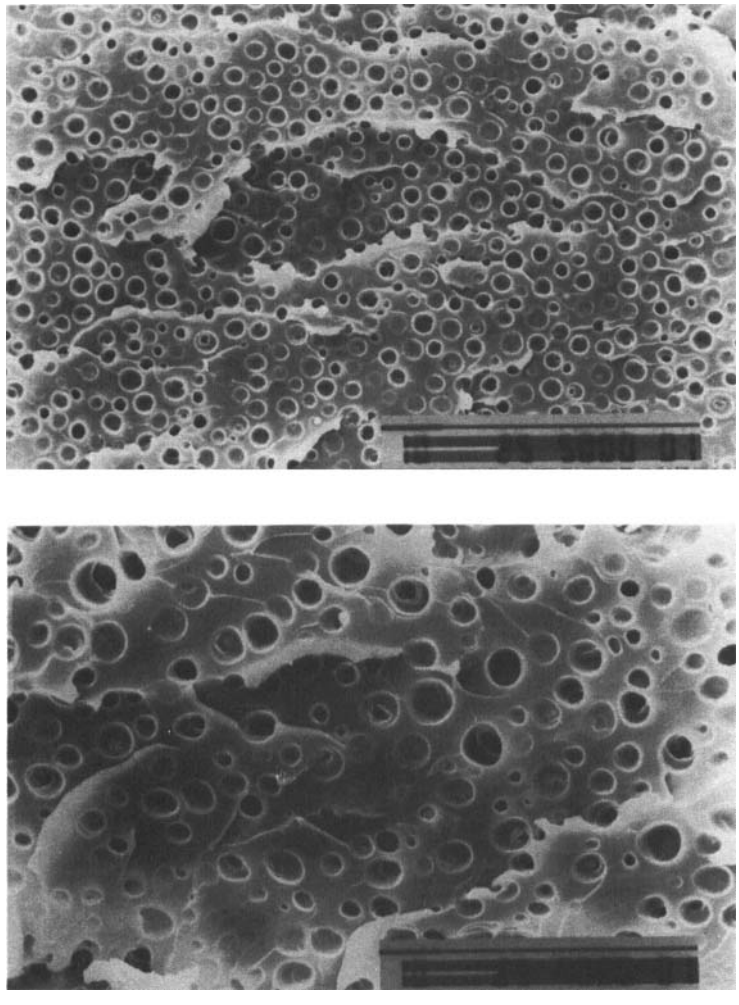

FIGURE 8 Scanning electron micrographs for the (a) 2*h* × 120°C and (b) 6*h* × 160°C systems.

from unfractured specimens. Detailed morphological studies are currently being conducted using this technique and will be discussed in a future publication.

Two major factors are now generally believed to have a major effect on the toughness of rubber-modified epoxies, these being rubber phase volume and matrix ductility.[6] Previous workers have quantified the matrix contribution in terms of T_g,[6] the assumption being that T_g will be dependent upon matrix structure which in turn will exert an influence on matrix ductility. Thus, by this reasoning, a low T_g would indicate a loose network structure which would result in a highly ductile matrix capable of taking full advantage of the stress-raising capacity of the rubber particles. Thus, from this argument, a rubber-modified epoxy comprising a low T_g matrix would exhibit a greater toughness than its higher T_g counterpart, all other morphological characteristics being equal. As previously indicated in Figure 7, no significant difference in T_g was observed between the two cure regimes. This was somewhat surprising since a significant matrix contribution to the substantial changes in G_{Ic} previously discussed would seem likely. However, it must be stressed that it is unlikely that matrix T_g alone would adequately quantify the matrix ductility contribution to toughness. Other factors will clearly be of importance since it is well known that polymers can exhibit high T_g values (in excess of 200°C) and still exhibit ductile behaviour.

Although precise morphological characteristics such as rubber-phase volume and average particle size are not yet available, the limited data presented suggests a contribution to the property variations obtained by these parameters. The significance of these contributions have however to be determined.

3.2 Adhesive joint properties

Figure 9 shows data previously obtained for adhesive joint G_{Ic} values obtained for the same adhesive system, cured for the traditional 16 hours at 120°C.[9] As

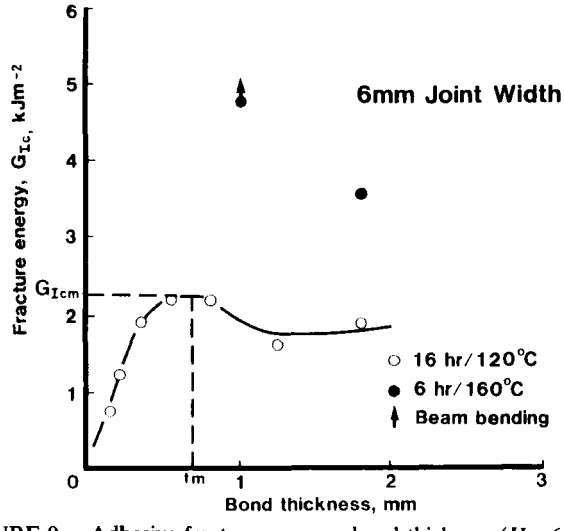

FIGURE 9a Adhesive fracture energy v bond thickness ($H = 6$ mm).

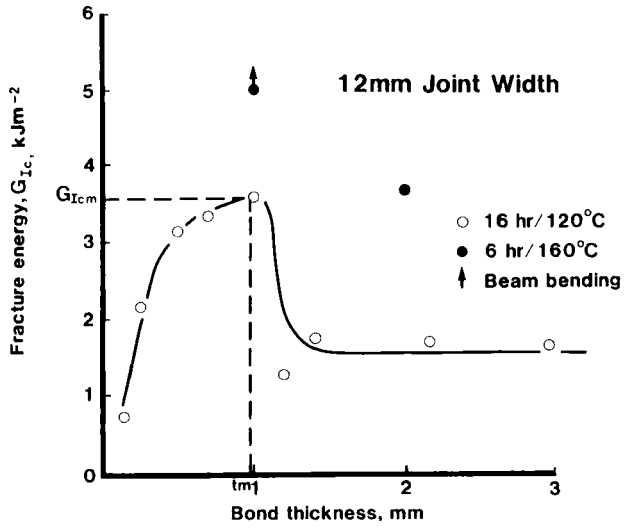

FIGURE 9b Adhesive fracture energy v bond thickness ($H = 12$ mm).

indicated, adhesive bond thickness has a significant effect on adhesive fracture energy. For each joint width, adhesive fracture energy G_{Ic}(joint), passes through a maximum, G_{Icm}, at a specific bond thickness, t_m. At thicknesses beyond t_m, G_{Ic} (joint) declines until a value is reached which remains essentially constant with increased thickness. Reasons for this bond thickness effect, together with the influence joint width has on the G_{Ic} (joint)-bond thickness relationship have been discussed in terms of a crack tip plastic zone restriction/constraint mechanism, the basis of which is demonstrated in Figure 10.[9,14] As indicated, the prime factor

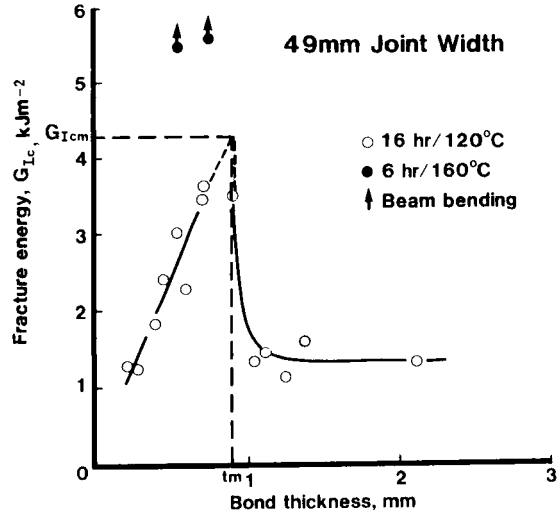

FIGURE 9c Adhesive fracture energy v bond thickness ($H = 49$ mm).

controlling G_{Ic}(joint) is the plastic zone volume. This, in turn, is influenced by two major factors. Firstly, due to the relatively large plastic zones prevalent with rubber-modified epoxies (the dimensions of which are of a similar magnitude to the bond thicknesses employed here) restriction of the development of the plastic zone, in the bond thickness direction, resulting in a reduction in plastic zone volume, is distinctly feasible. Since fracture energy is dependent on plastic zone dimensions any restriction on the development of the latter will result in a reduced toughness. Secondly, both finite element analytical techniques[22] and experimental observations[14] have indicated that an increase in the degree of constraint imposed on an adhesive layer by, for example, decreasing bond thickness, can increase significantly the distance over which the stresses giving rise to the plastic zone exist. This can result in an extension of the plastic zone along the bond line, thus resulting in an increased plastic zone volume.

As a result of these two effects, the maximum volume of crack tip plastic deformation in the adhesive layer occurs when $t_m = 2r_y$. That is, when the maximum degree of constraint exists, at a given bond thickness, commensurate with the condition that no restriction on the development of the plastic zone from the high modulus substrates exists. Under this situation, G_{Ic}(joint) will be at its maximum value, G_{Icm}. At $t < t_m$, a high degree of constraint will exist and thus the deformation zone will extend a considerable distance along the adhesive layer. However, restriction in the development of the zone in the bond thickness direction will also occur, with the overall effect of reducing plastic zone volume

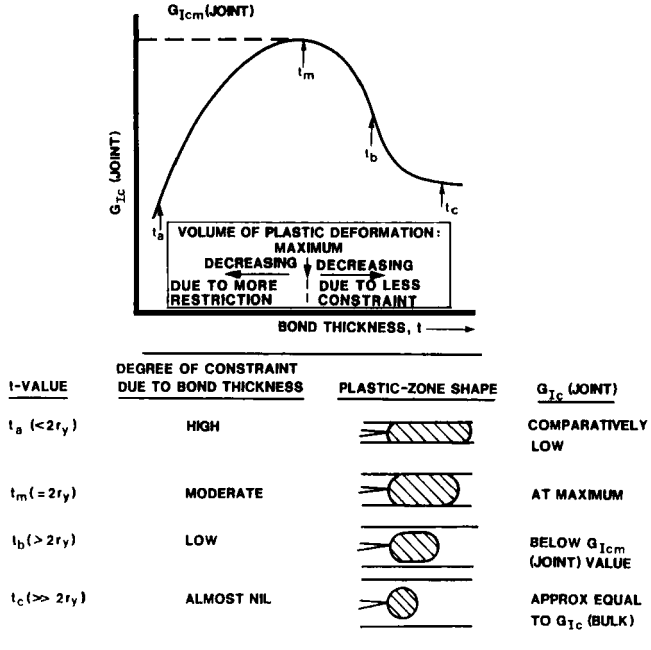

FIGURE 10 Crack tip plastic zone restriction/constraint mechanism (9).

and thus G_{Ic}. At $t > t_m$, restriction in the bond thickness direction will no longer apply, but constraint on the adhesive layer will decrease, thereby reducing zone length and consequently zone volume, thus reducing G_{Ic}. Furthermore, experimental results have shown that at bond thicknesses sufficiently large so that adhesive layer constraint is negligible, G_{Ic}(joint) is similar to values obtained from bulk monolithic specimens.[14]

Also included in Figure 9 are further fracture data obtained from cantilever beam specimens in which adhesive cured for 6 hours at 160°C was employed, *i.e.* the cure condition which promotes the maximum bulk toughness. For all three joint widths (6, 12 and 49 mm) the use of the more severe cure condition produces an enhanced G_{Ic}(joint), to the extent that in most cases permanent bending of the mild steel beams becomes the dominant failure mode, the crack in the adhesive layer remaining stationary throughout the test. Consequently, the attainment of detailed G_{Ic}-bond thickness profiles using this enhanced cure condition is not possible whilst the current substrates are employed. In the two cases where such bending was not observed, with ultimate failure occuring by crack growth through the adhesive layer, it is interesting to note that the G_{Ic} values obtained were somewhat lower than obtained from corresponding bulk specimens. Bearing in mind the bond thicknesses employed, the above mechanism and the bulk fracture data obtained, significantly higher G_{Ic}(joint) values would have been expected. The reason for this anomaly is currently unclear but may be associated with a combination of (a) difference in stress state between the two geometries employed (compact tension and contoured double cantilever beam) and (b) a reflection of the overestimate of some of the bulk G_{Ic} values, due to the plasticity-related effects previously discussed.

4 CONCLUSIONS

Experiments conducted on a piperidine-cured, rubber-modified epoxy adhesive have shown that cure conditions (temperature and time) have a major effect on mechanical properties. Fracture energy, G_{Ic}, has been shown to be particularly susceptible to variations in cure conditions, with increases in cure temperature from 120 to 160°C, resulting in remarkable increases in G_{Ic} in both bulk and adhesive joint form. Furthermore, substantial reductions in cure time from the traditional 16 hours has no adverse effect on properties. The reasons for these major effects would seem to be associated with morphological factors such as rubber phase volume and particle size together with matrix ductility. These are currently being studied in detail and will be reported in a later publication.

5 Acknowledgements

The authors would like to express appreciation to Mrs. M. Corthine for experimental assistance.

References

1. E. H. Rowe, A. R. Siebert and R. S. Drake, *Mod. Plast.* **49,** 110 (1970).
2. R. S. Drake, E. H. Rowe, A. R. Siebert and C. K. Riew, *Reinf. Plast.* **8,** (1971).
3. C. K. Riew, E. H. Rowe and A. R. Siebert in *Rubber Toughened Thermosets, Adv. Chem. Ser.* **184,** 326 (1976) (Am. Chem. Soc., Washington, DC).
4. A. C. Meeks, *Polymer* **15,** 675 (1974).
5. L. D. Manzione, J. K. Gillham and C. A. McPherson, *J. Appl. Polym. Sci.* **26,** 889 (1981).
6. L. C. Chan, J. K. Gillham, A. J. Kinloch and S. J. Shaw in *Rubber Modified Thermoset Resins, Adv. Chem. Ser.* **208,** 235 (1984) (Am. Chem. Soc., Washington, DC).
7. W. D. Bascom, R. L. Cottington, R. L. Jones and P. Peyser, *J. Appl. Polym. Sci.* **19,** 2545 (1975).
8. W. D. Bascom and R. L. Cottington, *J. Adhesion* **7,** 333 (1976).
9. A. J. Kinloch and S. J. Shaw, *ibid.* **12,** 59 (1981).
10. A. J. Kinloch, S. J. Shaw, D. A. Tod and D. L. Hunston, *Polymer* **24,** 1341 (1983).
11. A. J. Kinloch, S. J. Shaw and D. L. Hunston, *ibid.* **24,** 1355 (1983).
12. J. P. Knott, *Fundamentals of Fracture Mechanics* (Butterworths, London, 1973).
13. A. J. Kinloch and S. J. Shaw in *Developments in Adhesives 2,* A. J. Kinloch, Ed. (Applied Science, London, 1981), p. 82.
14. S. J. Shaw, Ph.D Thesis, City University, London, 1984.
15. A. J. Kinloch, C. A. Finch and S. Hashemi, *Polym. Comm.* **28**(12), 322 (1987).
16. J. B. Enns and J. K. Gillham, *J. Appl. Polym. Sci.* **28,** 2567 (1983).
17. V. B. Gupta, L. T. Drzal, C. Y.-C. Lee and M. J. Rich, *Polym. Eng. Sci.* **25**(13), 812 (1985).
18. E. Sancaktar, H. Jozavi and R. M. Klein, *J. Adhesion* **15,** 241 (1983).
19. J. G. Williams, *J. Appl. Polym. Sci.* **23,** 3433 (1979).
20. R. G. C. Arridge and J. H. Speake, *Polymer* **13,** 433 (1972).
21. T. Hirai and D. E. Kline, *J. Appl. Polym. Sci.* **17,** 31 (1973).
22. S. S. Wang, J. F. Mandell and F. J. McGarry, *Int. J. Fract.* **14,** 39 (1978).